THE JOURNAL OF BIOLOGICAL CHEMISTRY VOL. 288, NO. 6, pp. 4321–4333, February 8, 2013

Loss of Anterior Gradient 2 (*Agr2*) Expression Results in Hyperplasia and Defective Lineage Maturation in the Murine Stomach*

Received for publication, November 1, 2012, and in revised form, December 2, 2012 Published, JBC Papers in Press, December 3, 2012, DOI 10.1074/jbc.M112.433086

Aparna Gupta[‡], **Dariusz Wodziak**[‡], **May Tun**[‡], **Donna M. Bouley**[§], **and Anson W. Lowe**[‡1]

From the [‡]*Department of Medicine, Stanford University and the* [§]*Department of Comparative Medicine, Stanford University School of Medicine, Stanford, California 94305*

Background: The *in vivo* function of the adenocarcinoma-associated gene, *Agr2*, is not known in the stomach.
Results: *Agr2* KO mice displayed hyperplasia and defective cell maturation in the stomach.
Conclusion: *Agr2* expression promotes cell lineage differentiation and results in a negative feedback for cell proliferation.
Significance: *Agr2* functions in regulating homeostasis between differentiating and proliferating cells in the stomach.

Recent studies of epithelial tissues have revealed the presence of tissue-specific stem cells that are able to establish multiple cell lineages within an organ. The stem cells give rise to progenitors that replicate before differentiating into specific cell lineages. The mechanism by which homeostasis is established between proliferating stem or progenitor cells and terminally differentiated cells is unclear. This study demonstrates that *Agr2* expression by mucous neck cells in the stomach promotes the differentiation of multiple cell lineages while also inhibiting the proliferation of stem or progenitor cells. When *Agr2* expression is absent, gastric mucous neck cells increased in number as does the number of proliferating cells. *Agr2* expression loss also resulted in the decline of terminally differentiated cells, which was supplanted by cells that exhibited nuclear SOX9 labeling. *Sox9* expression has been associated with progenitor and stem cells. Similar effects of the *Agr2* null on cell proliferation in the intestine were also observed. *Agr2* consequently serves to maintain the balance between proliferating and differentiated epithelial cells.

The stomach functions to store, mechanically breakdown, and enzymatically digest food. It secretes acid that inactivates microbes and produces specialized secretory products such as mucins, pepsinogen, intrinsic factor, gastrin, and ghrelin. An assortment of cell types are specifically distributed throughout the organ to fulfill these multiple functions (1). The proximal third of the murine stomach, the forestomach (Fig. 1*A*), is lined by a stratified squamous epithelium and serves to store food (1). The lower two-thirds of the stomach represents the glandular stomach, which is divided into two sections, the corpus at the proximal end and the antrum at the distal end (Fig. 1*A*). The corpus encompasses gastric glands that contain different cell types and are divided into regions extending from the stomach lumen to the gland base. The pit layer contains pit cells (also known as foveolar cells) that line the superior aspect of each gastric gland and secretes mucin (Fig. 1*B*). Below the pit layer is the isthmus, where putative stem and progenitor cells that give rise to all gastric cell lineages reside (2–6). Differentiating cells from the isthmus migrate superiorly and inferiorly within the gastric gland to their final destinations. Below the isthmus is the neck layer containing mucous neck cells, which are precursors for the chief cells situated at the gland base that secrete pepsinogen and intrinsic factor (7–9). Mucous neck cells specifically express trefoil factor 2 (TFF2) and a secreted protein that binds the lectin *Griffonia simplicifolia* II (GSII)[2] (10–13). Acid-secreting parietal cells are distributed throughout the gastric gland below the pit layer, and the chief cells reside at the gland base. The distal half of the glandular stomach is the antrum, which contains mucous glands (Fig. 1*B*). Proliferating cells allegedly representing stem and progenitor cells in the antrum reside in the isthmus region just above the base of the antral gland. Mucin-secreting cells reside superiorly and inferiorly to the antral isthmus. Throughout the glandular stomach are isolated enteroendocrine cells that secrete a variety of products such as gastrin, ghrelin, somatostatin, and gastric inhibitory peptide.

Stem cells within the isthmus of the corpus and antrum contribute to all cell lineages within the glandular stomach. The means by which homeostasis is maintained between terminally differentiated cells and stem or progenitor cells are not known. In this study, the phenotype produced by an *Agr2* null mouse provides insights into its role in maintaining homeostasis.

Anterior gradient 2 (*Agr2*) is a gene that is widely expressed in human adenocarcinomas of the breast, lung, colon, pancreas, esophagus, ovary, prostate, and stomach (14–22). *Agr2* is highly conserved among vertebrates from amphibians to humans. The *Xenopus laevis* homologue of *Agr2, XAG2*, participates in the development of the cement gland and forebrain (23, 24). *Agr2* expression in salamanders serves an important

* This work was supported, in whole or in part, by National Institutes of Health Grant DK063624 (to A. W. L.).
The microarray data were deposited in the NCBI GEO database with accession number GSE40062.
[1] To whom correspondence should be addressed: Alway Bldg., Rm. M211, 300 Pasteur Dr., Stanford, CA 94305-5187. Tel.: 650-725-6764; Fax: 650-723-5488; E-mail: lowe@stanford.edu.

[2] The abbreviations used are: GSII, *G. simplicifolia II* lectin; EdU, 5-ethynyl-2′-deoxyuridine; GIF, gastric intrinsic factor; ER, endoplasmic reticulum; SPEM, spasmolytic protein expressing metaplasia; qRT, quantitative real-time; GIF, gastric intrinsic factor.

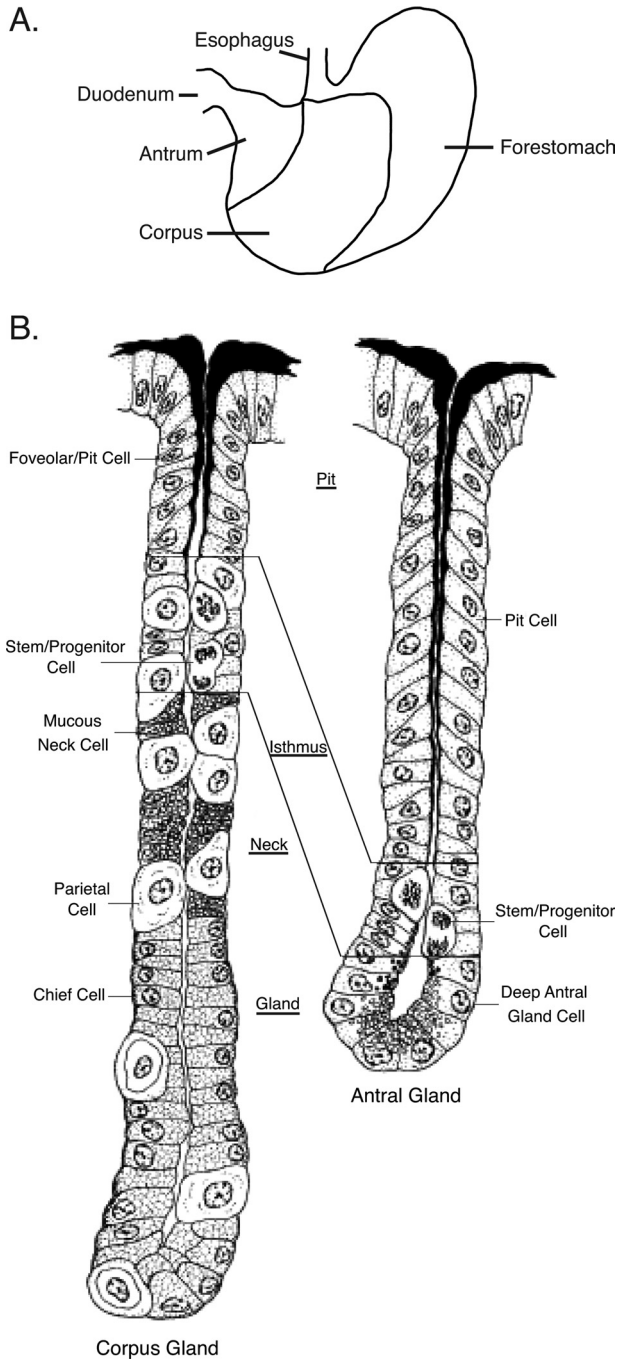

FIGURE 1. **Schematic of murine stomach anatomy and histology.** *A*, gross anatomy of the murine stomach is shown. The corpus and antrum comprise the glandular stomach. *B*, shown is a normal glandular structure showing the distribution of cell lineages in the corpus and antral glands. The figure is adapted from Lee (58). The material is reproduced with permission of John Wiley & Sons, Inc., New York.

role in nerve-dependent limb regeneration (25). Several studies have also demonstrated that *Agr2* supports many of the transformed properties of adenocarcinoma cell lines (26, 27). Potential mechanisms include activation of the Hippo signaling pathway through the co-activator *Yap1* and the induced expression of the EGF receptor ligand amphiregulin (28).

The present study explored the *in vivo* function of *Agr2* by generating a null mouse. The resultant mouse expressed a phenotype that was most pronounced in the stomach and was consistent with a role for *Agr2* in regulating cell proliferation, differentiation, and homeostasis among the different cell lineages in the mouse glandular stomach.

EXPERIMENTAL PROCEDURES

Generation of the Agr2 Null Mouse Model—The mouse, B6129S5-Agr2^{tm1Lex}, in which exons 2 to 5 were flanked by LoxP sites, was originally generated using 129SvEv^{Brd}-derived embryonic stem cells and bred on a 129/SvEv-C57BL/6 background. The mouse was obtained from Lexicon Pharmaceuticals (catalog no. LEXKO-2300). Exon 2 contains the start codon for AGR2 protein. *Agr2* null mice were produced by breeding the B6129S5-Agr2^{tm1Lex} mouse with another that constitutively expresses Cre recombinase, Tg$^{CMV\text{-}Cre}$ (B6.C-Tg(CMV-Cre)1Cgn/J, (The Jackson Laboratory, Bar Harbor, ME). Homozygous *Agr2*$^{-/-}$ mice (*Agr2* KO) were generated by breeding heterozygous *Agr2*$^{LoxP/WT}$;Tg$^{CMV\text{-}Cre}$. Female homozygous *Agr2*$^{-/-}$ bred poorly, which necessitated the heterozygous breeding.

A conditional *Agr2* null (*Agr2* KO) mouse in which excision of the floxed *Agr2* exons was achieved in adult mice after tamoxifen administration was generated by breeding the conditional B6129S5-Agr2^{tm1Lex} mice with a Cre^{ERT2} mouse (*Gt(ROSA)26Sor*$^{tm1(cre/ERT2)Tyj}$ (The Jackson Laboratory). Tamoxifen was administered to 8-week *Agr2*$^{LoxP/LoxP}$;*CMV-Cre*^{ERT2} mice by intraperitoneal injection at a dose of 75 mg/kg body weight for 5 consecutive days. The mice were then kept for an additional 21 days without tamoxifen before they were sacrificed. Controls consisted of *Agr2*$^{LoxP/LoxP}$ and *Agr2*$^{+/+}$ mice treated with tamoxifen in a similar manner. It should be noted that tamoxifen has been described to induce parietal cell apoptosis and an increase in gastric proliferation that is reversible after cessation of the drug (29). Experiments were performed that determined that proliferation returns to wild-type levels by 21 days after the last tamoxifen administration.

The care and use of animals was performed under the auspices of Stanford's Institutional Animal Care and Use Committee as approved under Stanford University's Animal Welfare Assurance (A3213-01).

Antibodies and Probes for Immunohistochemistry—Antibodies were kindly provided by the following individuals: anti-TFF2 by Lars Thim (Novo Nordisk A/S, Maløv, Denmark) (30); anti-gastric intrinsic factor by David Alpers (Washington University, St. Louis, MO); anti-ATP4A by Michael Caplan (Yale University, New Haven, CT). Other antibodies employed included: anti-AGR2 (Imgenex, San Diego, CA); anti-Ki-67 (catalog #M7249, DAKO, Carpinteria, CA); anti-SOX9 (EMD Millipore, Billerica, MA); anti-MUC5AC (catalogue #MS-145-P0, Thermo Fisher Scientific, Kalamazoo, MI). The lectin, GSII, was obtained from Vector Laboratories, Inc. (Burlingame, CA).

Labeling of proliferating cells was achieved by the intraperitoneal injection of the nucleotide analog, 5-ethynyl-2′-deoxyuridine (EdU) at a dose of 10 μg/g of mouse body weight 2 h before sacrificing the mice (31). Visualization of the incorporated EdU was achieved with the Click-iT® EdU Alexa Fluor® 488 Imaging kit (Invitrogen).

Immunohistochemistry—Slides were deparaffinized by immersing in xylene twice for 5 min each and hydrated by

immersing for 2 min each in a series of 100, 80, and 50% ethanol and finally in distilled H_2O. Slides for histological analysis were stained with hematoxylin and eosin by standard methods, with generally 3–4 sections reviewed per specimen. For immunofluorescence or immunohistochemistry, antigen retrieval was performed in a pressure cooker set to 118 °C for 3 min and removed at 90 °C in antigen unmasking solution (DAKO) followed by equilibration at room temperature for 1 h. Endogenous peroxidase activity was then blocked with freshly made 1.5% H_2O_2 for 30 min followed by washing in PBS (pH 7.4). The slides were placed in 5% serum blocking solution (goat, horse, or rabbit serum as appropriate) for 30 min to block nonspecific binding of antibody to the tissue. The sections were incubated with primary antibody diluted in 2% serum overnight at 4 °C. The dilutions used for each primary antibody used were AGR2 (1:250), synaptophysin (1:500), TFF2 (1:1000), gastric intrinsic factor (1:100), MUC5AC (1:500), Sox9 (1:1000), and Ki-67 (1:50). The respective secondary antibodies were used at a dilution of 1:300. Staining was visualized using Vectastain ABC kit (Vector Laboratories) for immunohistochemistry. Slides were counterstained with Gill No. 3 hematoxylin. Immunofluorescence slides were mounted with Vectashield mounting media containing DAPI (Vector Laboratories). Labeling with biotinylated GSII (Vector Laboratories) was performed at 10 μg/ml after blocking for 30 min with Carbo-free solution (Vector Laboratories).

DNA Microarray—Total RNA was extracted from fresh whole mouse stomachs using TRIzol reagent (Invitrogen). The RNA was reverse-transcribed, labeled, and hybridized to mouse oligonucleotide DNA microarrays (MouseRef-8 v2 Expression BeadChip, Illumina, San Diego, CA). Each array was normalized using the GenePattern software suite Version 3.3.3 (32, 33). The microarray data were deposited in the NCBI GEO database with accession number GSE40062.

RNA Extraction and qRT-PCR—Total RNA was isolated from tissues using TRIzol® reagent (Invitrogen). The glandular stomach was divided into the corpus and antrum, and 3 μg of total RNA from each was used to make cDNA. First-strand cDNAs were synthesized using Superscript II reverse transcriptase (Invitrogen) with random hexamer primers. Quantitative RT-PCR reactions were performed using IQ SYBR Green Supermix and the iCycler iQTM detection system (Bio-Rad). The primers used include: *Actb*, 5-GGCTGTATTCCCCTCCATCG-3, 5-CCAGTTGGTAACAATGCCATGT-3; *Atp4a*, 5-ATCTGCCTCATTGCCTTTGCCATC-3, 5-GTGACCACAACCACAGCAATGAGT-3; *Atp4b*, 5-ACTACTGTTGGAACCCGGACACT-3, 5-ATAGATGCACAAGGCAAAGAGCCC-3; *Chga*, 5-TGCTGAAGGAACTTCAAGACCTGG-3, 5-ATCCTCAAAGCTGCTGTGTTGCTG-3; *Chgb*, 5-CCAAGTCCAGTGTTCCAACGATCA-3, 5-CTGGGTCTCTTAGCAACCGTACTT-3; *Gast*, 5-TGGAACAGCGCCAGTTCAACAA-3, 5-TTCTTCTTCCTCCATTCGTGGCCT-3; *Ghrl*, 5-AGGAATCCAAGAAGCCACCAGCTA-3, 5-ATGCCAACATCGAAGGGAGCATTG-3; *Gif*, 5-CAGCATCCTGATTGCCATGAACCT-3, 5-ACACTTTACTTCCAGGGTCTCTGC-3; *Herpud1*, 5-ACCGCAGTTGGAGTGTGAGT-3, 5-TGATCCAACAGCAGCTTCCCAGAA-3; *Hspa5*, 5-AGACTGCTGAGGCGTATTTGGGAA-3, 5-AGCATCTTTGGTTGCTTGTCGCTG-3; *Muc5ac*, 5-TGGAAGGCAGTACACAGTACATGG-3, 5-TGGAAGGCAGTACACAGTACATGG-3; *Pgc*, 5-AAACCGGCATCATGAAGTGGATGG-3, 5-TTGTTCCTTCATGGTCTCCCGGAT-3; *Reg1*, 5-AGGAAGCTGAAGAAGACCTGCCAT-3, 5-AGAACTGACACCAGGTAGCCTGAA-3, *Reg3b*, 5-GCTCAATAGCGCTGAGGCTTCATT-3, 5-CTTGACAAGCTGCCACAGAAAGCA-3; *Reg3g*, 5-TGCCTATGGCTCCTATTGCTATGC-3, 5-CCACTGAGCACAGACACAAGATGT-3; *Sox9*, 5-CCACATTCCTCCTCCGGCAT-3, 5-TCGCTTCAGATCAACTTTGCCAGC-3; *Sst*, 5-GCTCTGCATCGTCCTGGCTTT-3, 5-AGTACTTGGCCAGTTCCTGTTTCC-3; *Tff2*, 5-ACCTGATCTTTGAAGTGCCCTGGT-3, 5-AAACTTTCTTCTGGCTTGCAGCTCCC-3.

RESULTS

Agr2 KO Mice Exhibited Enlarged Stomachs and Die Prematurely—A conditional $Agr2^{LoxP/LoxP}$ mouse with LoxP sites flanking exons 2–5 of the *Agr2* gene was generated to explore the gene function *in vivo* (Fig. 2*A*). Mating the $Agr2^{LoxP/LoxP}$ mouse with a mouse that constitutively expresses Cre recombinase in all cells resulted in $AGR2^{-/-}$ (*Agr2* KO) progeny (Fig. 2*B*). Homozygous $Agr2^{-/-}$ mice were viable at birth and appeared to undergo normal development. Immunohistochemistry and qRT-PCR revealed no evidence of *Agr2* expression in the stomach or any other tissue (Fig. 2*C*). After 12 weeks of age, however, the weight of the *Agr2* KO mice began to lag behind their wild-type (WT) controls (Fig. 2*D*), which was associated with signs of progressive morbidity that necessitated euthanasia (Fig. 2*E*). Autopsies revealed massively enlarged stomachs with large amounts of retained food (Fig. 2*F*). The presentation was consistent with gastric outlet obstruction due to pronounced mucosal hyperplasia in the antrum, which precluded the transport of food into the intestine. In addition to weight loss, other signs of poor nutrition included the loss of fat pads, hypoalbuminemia, and anemia.

The entire glandular epithelium, including the corpus and antrum, was grossly thickened (Fig. 2*G*). Eighteen-week-old *Agr2* KO mouse stomachs averaged 5 times heavier than their wild-type littermates (Fig. 2*H*). The small and large intestine also appeared larger than the wild-type controls (Fig. 2*F*). Thus *Agr2* loss resulted in reduced body weight, enlarged stomachs, thickening of the glandular mucosa, and premature death due to intestinal obstruction.

Agr2 Expression in the Wild-type Murine Stomach—Immunohistochemistry of the adult *Agr2* WT murine stomach revealed AGR2 protein expression in the corpus neck and the base of antral glands (Fig. 2*C*; see Fig. 4*A*). Within the wild-type glands, AGR2-positive cells were co-labeled with anti-TFF2 antisera and the lectin, GSII, both of which are established markers for mucous neck cells (see Fig. 4, *A* and *B*) (10, 12, 34). Cells at the base of the mucous glands in the antrum were also positive for AGR2, GSII, and TFF2 in *Agr2* WT mice (Figs. 4, *A* and *C*). *Agr2*, *Tff2*, and GSII are thus expressed in mucous neck cells and deep antral gland cells in the *Agr2* WT glandular stomach. *Agr2* expression was not detected in any other cell type in the stomach.

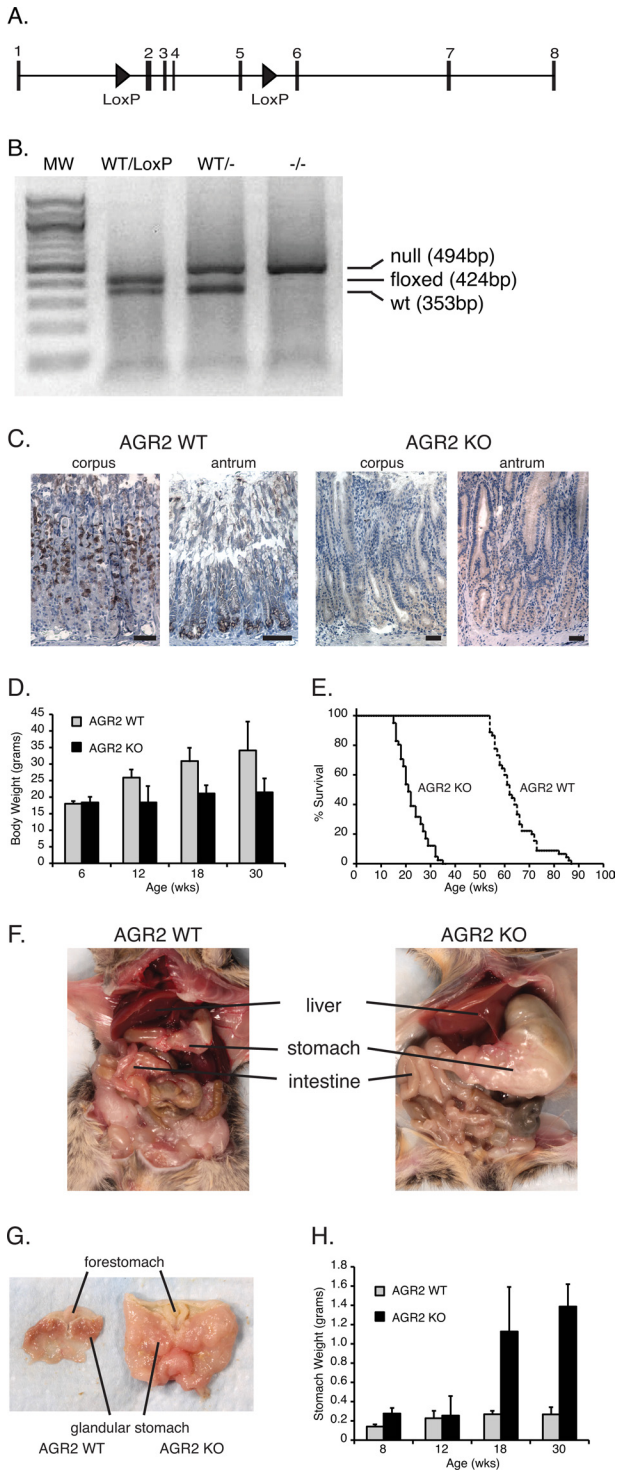

FIGURE 2. ***Agr2* KO mice phenotype.** *A*, shown is a schematic of the *Agr2* gene on chromosome 12 that encompasses 11,176 base pairs. The LoxP sites (*triangles*) flank exons 2 and 5. The ATG start site is in exon 2. *B*, PCR genotyping of $Agr2^{WT/LoxP}$, $Agr2^{WT/-}$, and $Agr2^{-/-}$ (null) is shown. C, immunohistochemistry of AGR2 expression in the corpus and antrum of *Agr2* WT and *Agr2* KO mice is shown. The *black scale bar* represents 20 μm. *D*, shown is average body weight at different ages for *Agr2* WT ($n = 29$) *versus Agr2* KO ($n = 16$). *Error bars* represent 1 $\pm$ S.D. *E*, shown is a survival curve for *Agr2* WT (*solid line*; $n = 88$) *versus Agr2* KO (*dashed line*; $n = 37$). *F*, shown is a representative image of the abdominal cavity for each mouse genotype at 26 weeks. *G*, shown are representative images of the stomach for each genotype. *H*, shown is stomach weight at different ages for *Agr2* WT ($n = 29$) *versus Agr2* KO ($n = 16$). *Error bars* represent $\pm$ 1 S.D. Differences in survival, body weight, and stomach weight are significant with $p < 0.0001$ for all pairs.

Agr2 KO Develops Hyperplasia in the Glandular Stomach—The histology of *Agr2* KO stomachs at 6 and 16 weeks revealed progressive mucosal hyperplasia of the corpus and antrum (Fig. 3). There was no evidence of tumor formation or extension of the hyperplasia through the muscular layers or serosa.

Review by a pathologist revealed no evidence of inflammatory infiltrates in the mucosa. There was mild inflammatory infiltration of the submucosa and muscular layers that was determined to be an unlikely cause of the changes within the glandular epithelium.

Expansion of Tff2- and GSII-expressing Mucous Neck Cells—Cell lineages are normally established and appropriately located in the murine stomach by 3 weeks, and by 6 weeks the mucosa has achieved its full thickness (5, 6, 12). Stomachs from 6-week-old mice were labeled with GSII lectin and anti-TFF2 antisera to evaluate the effects of *Agr2* loss on mucous neck cells. *Agr2* KO mice at 6 weeks displayed a significant increase in the number of TFF2- and GSII-labeled cells in the corpus and antrum compared with *Agr2* WT aged-matched controls (Fig. 4, *B* and *C*). In the corpus, TFF2/GSII-labeled cells extended beyond their normal location in the neck to the gland base (Fig. 4*B*). In the antrum, TFF2/GSII-labeled cells extended beyond their normal location at the gland base toward the lumen (Fig. 4*C*), which was most significant in areas of significant hyperplasia (Fig. 4*D*). *Agr2* loss thus results in prominent expansion of TFF2/GSII-positive cells.

Maturation Defect of Chief Cells and Loss of Parietal Cells in Agr2 KO Mice—The gastric glands are poorly developed in the murine stomach at birth (12). At this stage the stomach is essentially a tube with invaginations representing the developing gastric glands, and gastric intrinsic factor (*Gif*), a marker for chief cells, is co-expressed with the mucous neck cell marker, GSII, at the bottom of the developing gland. As the gastric glands develop the two markers segregate into different cells. By 3 week, GSII and GIF are segregated into two different cell types that have located to their respective locations in the neck and gland base, respectively (Fig. 4*E*). In contrast, 3-week-old *Agr2* KO mice displayed co-localization of GSII and GIF at the gland base, which was also observed for *Agr2* KO mice at the ages of 6, 12, and 24 weeks (data not shown), indicating that the chief cells never mature. Immunofluorescence intensity also revealed decreased GIF expression by chief cells in the *Agr2* KO mice (Fig. 4*E*). Quantitative RT-PCR of gastric corpus mRNA for *Gif* revealed a 6.7-fold decrease in *Agr2* KO mice compared with *Agr2* WT controls (Table 1).

Although parietal cells appeared to be abundant at 6 weeks of age, their numbers declined by 16 weeks in *Agr2* KO mice as determined by histology and immunohistochemistry (Figs. 3 and 4*F*). Quantitative RT-PCR of a 16-week-old *Agr2* KO mouse stomach confirmed a greater than 20-fold decrease in transcript levels for the H^+:K^+-ATPase subunits *Atp4A* and *Atp4B*, which are specifically expressed by parietal cells (Table 1).

Decreased Expression of Pit and Enteroendocrine Cell Markers—Pit cells in the glandular stomach are responsible for mucin secretion, which can be detected with antibodies against the secretory mucin MUC5AC. *Agr2* KO mice displayed decreased MUC5AC staining intensity compared with *Agr2*

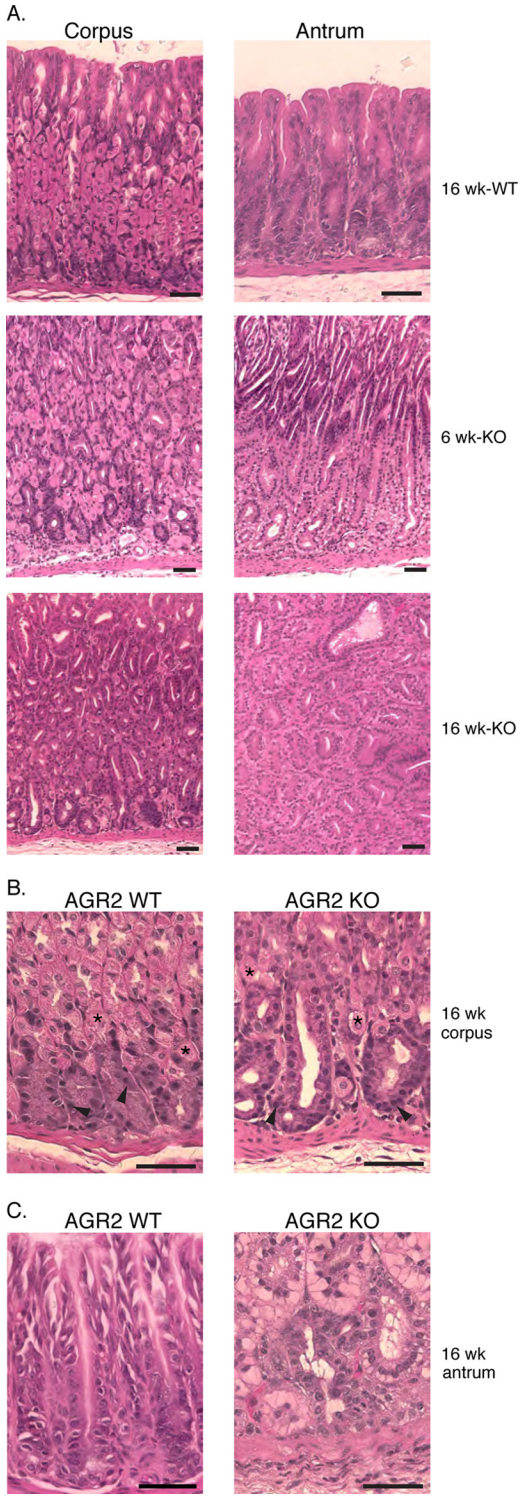

FIGURE 3. **Gastric Histology of *Agr2* WT and *Agr2* KO mice.** *A*, corpus and antrum of *Agr2* WT mice at 16 weeks and *Agr2* KO mice at 6 and 16 weeks are shown. The *brackets* at 6 weeks mark the expanding zone of clear cells in the antrum above the lamina propria. *B*, shown is high magnification of the corpus gland base containing chief and parietal cells in *Agr2* WT and *Agr2* KO mice. Representative parietal cells are marked with *asterisks*, and chief cells are marked with *arrowheads*. *C*, high magnification of the antral gland base is shown. The *black scale bars* represent 50 μm.

WT mice in the corpus (Fig. 5*A*). The total number of MUC5AC-positive cells, however, increased in the *Agr2* KO. Quantitative RT-PCR of 16-week-old *Agr2* KO mice detected a 5- and 9-fold decrease in *Muc5ac* transcript levels in the corpus and antrum, respectively (Table 1). In the antrum, intense periodic acid-Schiff staining, which is a characteristic of neutral mucins such as MUC5AC, was observed above the isthmus in the antrum of *Agr2* WT mice. In contrast, periodic acid-Schiff staining of cells in the *Agr2* KO antrum decreased dramatically, but again the number of positively labeled cells increased. Cells at the base of antral glands in *Agr2* WT mice stained with Alcian blue, which is characteristic of acidic mucins. Alcian blue staining was absent in the *Agr2* KO mice (Fig. 5*B*).

Enteroendocrine cells were affected in 16-week-old *Agr2* KO mice as qRT-PCR of gastric RNA detected a 3- and 5-fold decrease in the transcript levels for ghrelin and somatostatin, respectively. Similar decreases in transcripts levels were detected for the general endocrine biomarkers chromogranin A (*Chga*, 8-fold) and chromogranin B (*Chgb*, 2.7-fold) (Table 1). Despite the low numbers of parietal cells, which normally induces an increase in gastrin synthesis, gastrin transcript levels in the 16-week-old *Agr2* KO mice antrum were 20% lower than *Agr2* WT controls (Table 1). No significant changes were observed in pit or enteroendocrine markers in 6-week-old *Agr2* KO mice (Table 1). In summary, pit cell and enteroendocrine cell lineage marker expression declines with age.

Increased Cell Proliferation in Agr2 KO Mice—In view of the glandular hyperplasia observed in the stomach, an assessment of cell proliferation and apoptosis was performed. TUNEL assays of *Agr2* WT and *Agr2* KO mice revealed no apoptosis in the stomachs of either group (data not shown). Two different assays were used to assess cell proliferation. One approach utilized the injection of a nucleotide analog, EdU followed by its detection with immunofluorescence (31). A second approach utilized Ki-67 antisera, which is a biomarker for actively cycling cells (35). Consistent with previous studies (2), EdU-labeled cells were detected in the isthmus of the *Agr2* WT corpus and antrum (Fig. 6*A*). *Agr2* KO mice displayed a 3.8- and 2.5-fold increase in EdU-labeled cells in the corpus and antrum, respectively, compared with *Agr2* WT mice (Fig. 6*B*).

Induced Agr2 Loss in Adult Mice Also Affects Cell Proliferation—Embryonic loss of *Agr2* in the constitutive *Agr2* KO mouse could potentially affect development to produce the findings described. Therefore, 8-week-old adult $Agr2^{LoxP/LoxP}$; $CMV\text{-}Cre^{ERT2}$ mice were injected with a 5-day course of tamoxifen to induce Cre recombinase activity and sacrificed 21 days after the last dose. *Agr2* KO mice exhibited a 3- and 5-fold decrease in AGR2-labeled cells in the corpus and antrum, respectively, compared with the control $Agr2^{LoxP/LoxP}$ mice that were also treated with tamoxifen in a similar manner (Fig. 6, *C* and *D*). Immunohistochemistry for Ki-67-labeled nuclei revealed a 1.5- and 3.3-fold increase in cell proliferation in the corpus and antrum, respectively, compared with the control. The loss of *Agr2* expression in adult mice thus results in increased cell proliferation in the corpus and antrum of the glandular stomach.

A recently reported adverse effect of tamoxifen is reversible parietal cell loss, metaplasia of chief cells, and increased cell proliferation (29). The tamoxifen-induced effects reverted to base line 21 days after a single dose of tamoxifen. The metaplasia previously described was characterized by TFF2 and GSII

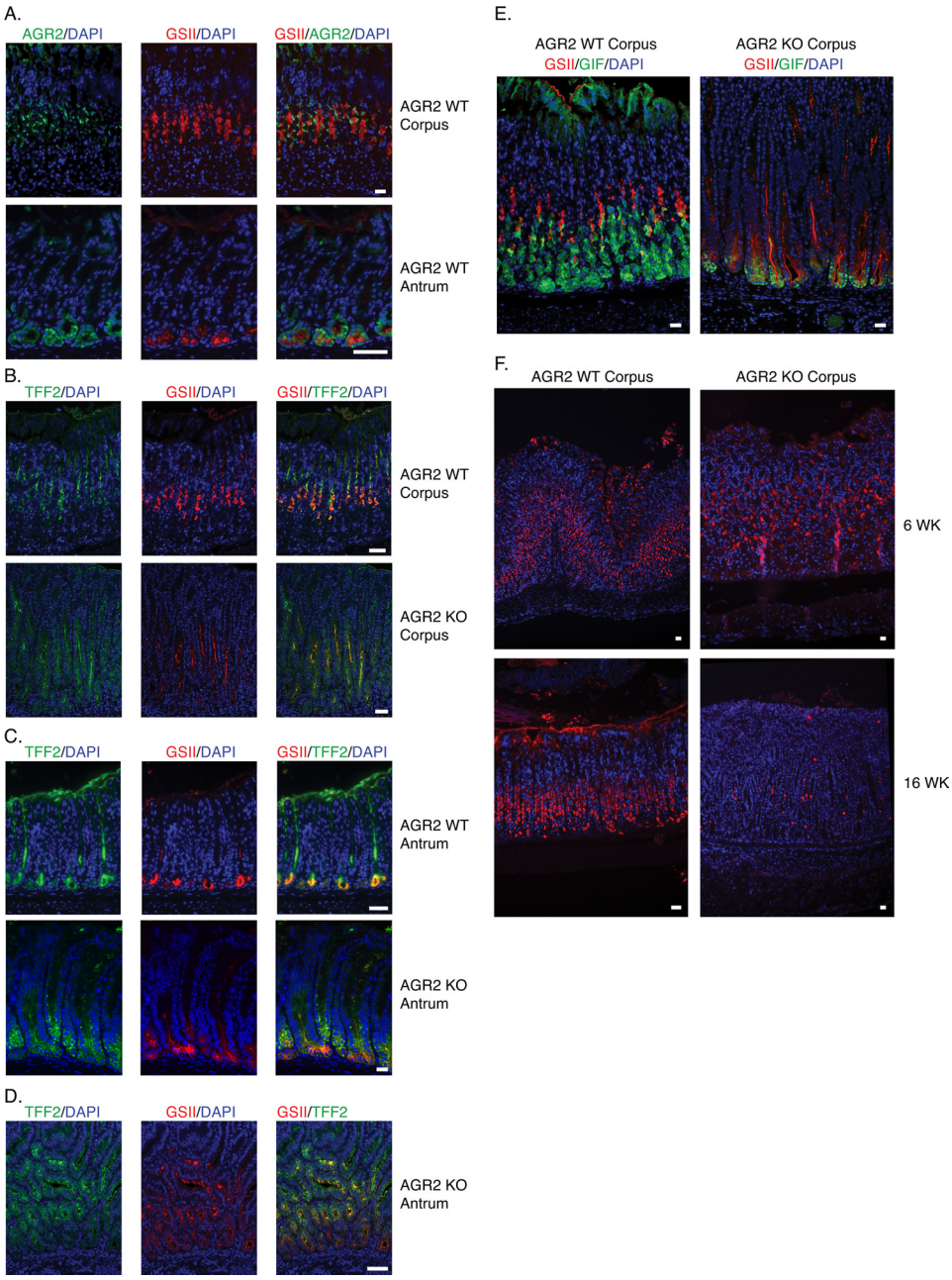

FIGURE 4. **Mucous neck, chief, and pit cell markers in *Agr2* WT and *Agr2* KO mice.** *A*, shown is *Agr2* WT gastric corpus and antrum labeled with anti-AGR2 antisera (*green*) and the mucous neck cell marker, GSII lectin (*red*). *B* and *C*, shown is double-labeling with anti-TFF2 antisera (*green*) and GSII lectin (*red*) of *Agr2* WT and *Agr2* KO mice in the corpus (*B*) and antrum (*C*). *D*, shown is an area of pronounced antral hyperplasia. Data were obtained from 6-week-old mice (*A–C*) and from a 16-week-old *Agr2* KO mouse (*D*). *E*, shown are 3-week-old *Agr2* WT and *Agr2* KO corpus labeled with anti-gastric intrinsic factor (*green*) and GSII lectin (*red*). *F*, shown is labeling of *Agr2* WT and *Agr2* KO corpus at 6 and 16 weeks with anti-ATP4A antisera that binds a H^+:K^+-ATPase subunit specifically expressed by parietal cells. Nuclei are stained *blue* with DAPI. All *scale bars* represent 25 μm.

labeling at the gastric gland base, similar to what was observed in the *Agr2* KO. *Agr2* WT controls that possessed a floxed *Agr2* but without Cre recombinase activity were evaluated for AGR2 protein expression and proliferation with immunohistochemistry. As demonstrated in the previous aforementioned study, cell proliferation returned to base line 21 days after tamoxifen administration. Similar to the previous study, parietal cell numbers returned, but there was still residual GSII and TFF2 labeling at the gland base (data not shown). Labeling for AGR2 protein was also detected at the gland base in addition to the neck region (Fig. 6*C*).

A Fraction of GSII Labeled Cells Are Proliferating in Agr2 KO Mice—Proliferating cells labeled for 2 h with EdU were evaluated for co-expression of ATP4A (parietal cells), MUC5AC (pit cells), and GIF (chief cells) in the *Agr2* KO mice (Fig. 7, *A–C*). None of the proliferating cells was found to express markers consistent with the differentiated cell types. In contrast, 37 and 24% of proliferating EdU-labeled cells in the corpus and antrum, respectively, co-labeled with the mucous neck cell marker GSII in *Agr2* WT mice, which increased to 53 and 43% in *Agr2* KO mice (Fig. 6*A*). An assessment of proliferating AGR2-expressing cells in *Agr2* WT mice was determined using

TABLE 1
qRT-PCR of stomach RNA

RNA was extracted at 6 and 16 weeks of age from the corpus and antrum of *Agr2* WT and *Agr2* KO mice. The results are expressed as a ratio of the KO to the WT. – signifies no significant expression from which to assess a ratio.

	qRT-PCR of RNA from the corpus and antrum (null/WT)			
	6 Weeks old		16 Weeks old	
Gene	Corpus	Antrum	Corpus	Antrum
Pitt cell				
MUC5AC	1.04	1.41	0.11	0.20
Parietal cell				
ATP4A	0.71	–	0.049	–
ATP4B	0.95	–	0.042	–
Chief cell				
PGC	1.32	–	0.33	–
GIF	0.87	–	0.15	–
Mucous neck cell				
TFF2	0.97	0.66	6.28	2.64
Enteroendocrine				
CHGA	1.10	0.81	0.13	0.13
CHGB	1.11	0.31	0.37	0.37
GAST	–	0.29	–	0.84
GHRL	0.84	–	0.32	–
SST	1.41	2.07	0.23	0.07
ER stress				
HERPUD1	1.05	2.10	1.46	0.65
HSPA5	0.98	1.62	1.80	1.15
Growth factors				
REG1	0.54	0.54	36.76	100.43
REG3B	0.49	0.73	66.26	207.94
REG3G	0.90	0.44	71.01	247.28
Miscellaneous				
SOX9	1.54	1.25	3.61	1.57

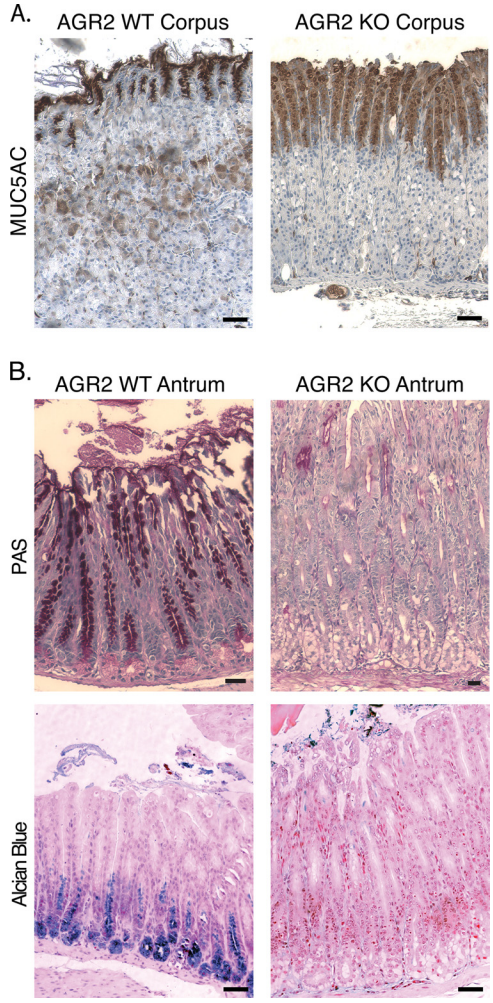

FIGURE 5. **Mucus Declines in *Agr2* KO mice.** *A*, shown is MUC5AC immunohistochemistry of the corpus in *Agr2* KO *and* WT mice. *B*, shown is staining in the antrum for neutral (periodic acid-Schiff (PAS), *top row*) and acid (Alcian blue, *bottom row*) mucins in *Agr2* KO and WT mice. All *scale bars* represent 50 μm.

double immunofluorescence for AGR2 and EdU (Fig. 7*D*). After a 2-h labeling with EdU of *Agr2* WT mice, 16 and 14% of the EdU-positive cells were also positive for AGR2 in the corpus and antrum, respectively. In summary, parietal, pit, and chief cell cells were not proliferating. There is a fraction of proliferating GSII-positive cells that may account for the TFF2/GSII expanded cell population in the *Agr2* KO.

Sox9 Is Co-expressed by TFF2/GSII-labeled Cells in Agr2 WT and Agr2 KO Mice—Recent studies have suggested increased *Sox9* expression in mucous neck cells, gastric intestinal metaplasia, and gastric adenocarcinoma in humans (36). *Sox9* has been associated with stem cells and pluripotent, mitotically active progenitor cells in a wide variety of organs that include the pancreas, intestine, and liver (37, 38). Other studies have shown *Sox9* to be necessary for initiating differentiation (39, 40).

Nuclear SOX9 protein in *Agr2* WT mice was detected by immunohistochemistry in the isthmus of the gastric corpus and the base of the antral glands (Fig. 8*A*). SOX9 co-localized with GSII-labeled cells in the *Agr2* WT. In the *Agr2* KO, SOX9- and GSII-co-labeled cells increased dramatically in both the corpus and antrum (Fig. 8*A*). Quantitative RT-PCR revealed a 3.6- and 1.6-fold increase in *Sox9* transcript levels in the corpus and antrum, respectively (Table 1). A small fraction of nuclear-labeled SOX9 cells was also co-labeled with the proliferation antigen, Ki-67 (Fig. 8*B*). *Agr2* WT mice thus express SOX9 in mucous neck cells and deep antral gland cells. In the absence of AGR2, there is an expansion of SOX9-positive cells that is also GSII-positive.

The Small and Large Intestine Also Exhibit Enhanced Proliferation and SOX9 Expression in the Agr2 KO—Gross inspection of the small intestines revealed that they were enlarged (Fig. 2), which was verified by their increased weight in older mice. No significant difference in small intestine weight was observed at less than 12 weeks of age. For *Agr2* KO mice greater than 24 weeks of age, the mean weight was 2-fold higher when compared with WT (1.9 *versus* 1.1, p value $= 4.6 \times 10^{-9}$) or heterozygotes (1.9 *versus* 1.1, p value $= 4.8 \times 10^{-7}$) (Fig. 9*B*).

Two previous studies have reported the generation of *AGR2* null mice whose major phenotype was reduced mucin production in intestinal goblet cells (41, 42). Immunohistochemical analysis of the *Agr2* KO mouse intestine described in this study also revealed decreased mucin production by the small intestine (Fig. 9*A*). Alcian-blue staining goblet cells were present, but the signal intensity in each cell was dramatically reduced.

Further analysis of the histology revealed no signs of abnormal inflammation in the *Agr2* KO intestines. There were no signs of infiltration by inflammatory cells into the mucosa, submucosa, or muscular layers.

Similar to the previous analysis of the stomach, nuclear SOX9 expression and cell proliferation was also determined in the intestines (Fig. 9*D*). The increase in DAPI-, Ki-67-, and SOX9-labeled nuclei per crypt was 1.7-, 2.1-, and 2.3-fold, respectively, in *Agr2* KO compared with *Agr2* WT mice (Fig. 9*C*). Ki-67 labeling was largely absent from the intestinal crypt bottoms where stem cells arise but enhanced in a crypt region usually associated with progenitor cells. Similar to the stomach,

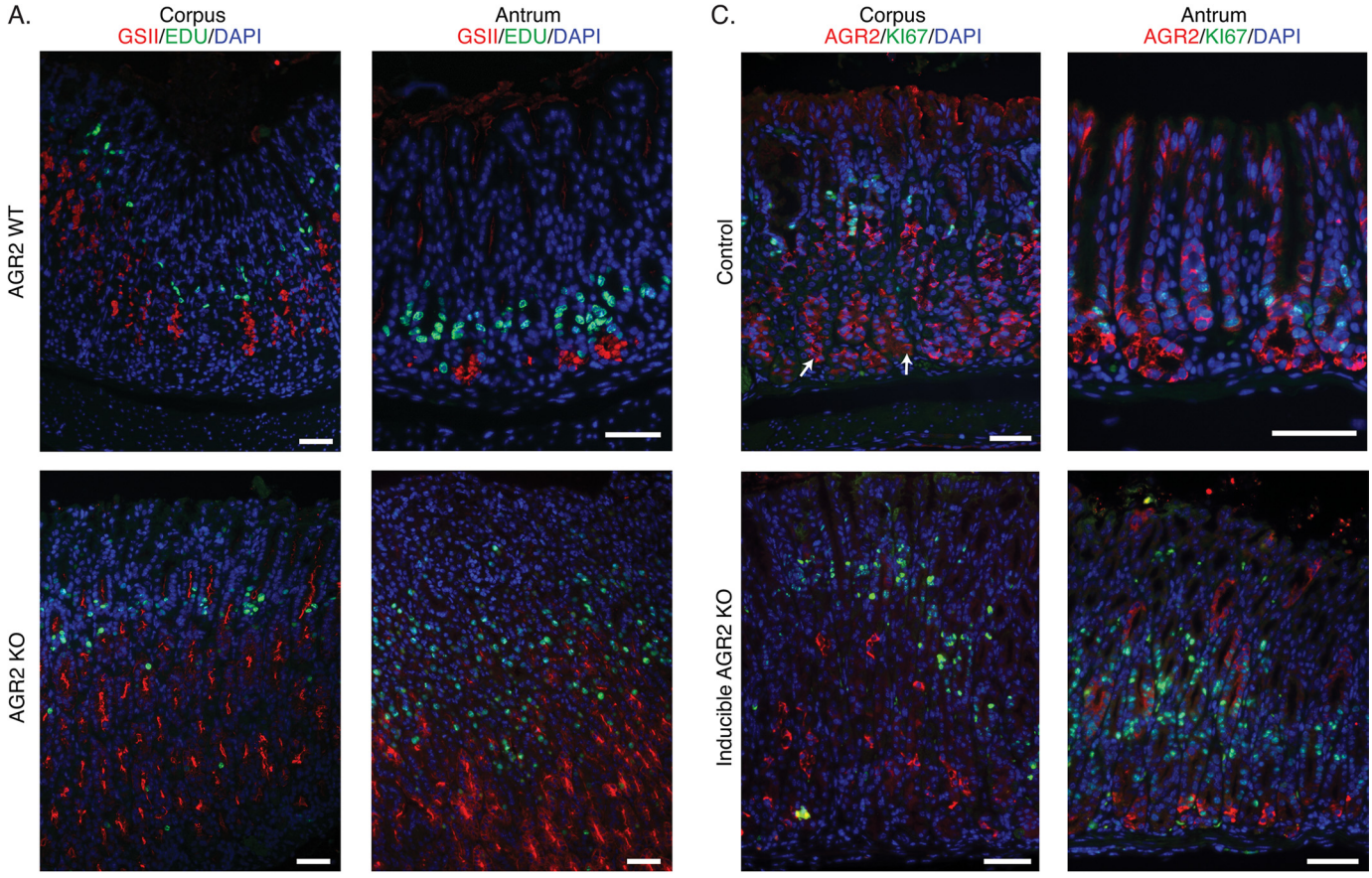

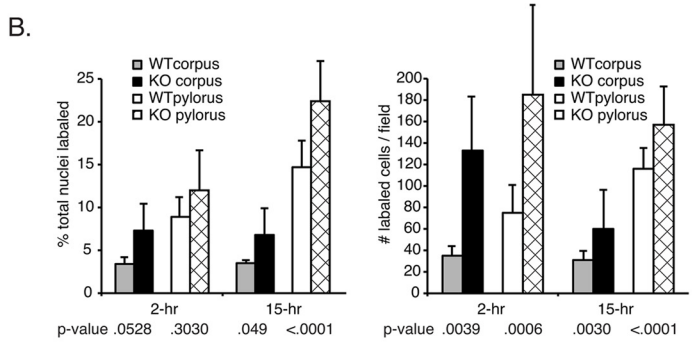

Total number of nuclei counted

	2-hr	15-hr
WT corpus	4002	3533
KO corpus	5435	3502
WT pylorus	4257	3513
KO pylorus	6158	2805

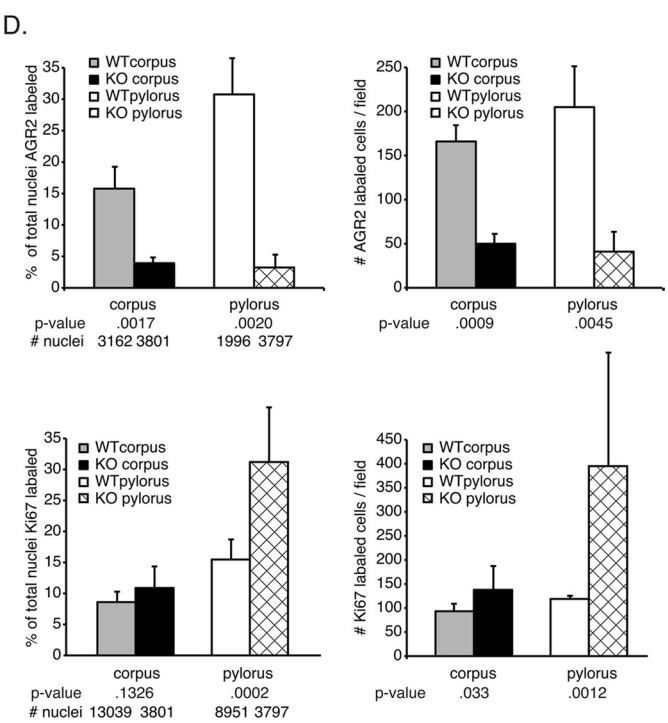

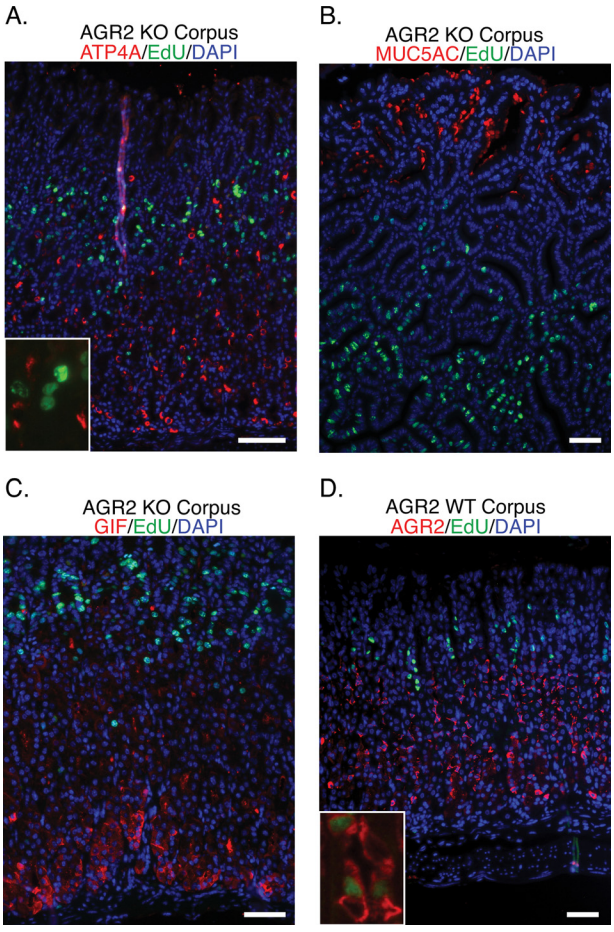

FIGURE 7. **Proliferating cells in *Agr2* KO do not label with differentiated lineage markers.** *Agr2* KO mice (*A–C*) were sacrificed 2 h after injection with EdU (*green*) and labeled for the following cell markers: *A*, ATP4A, a parietal cell marker (*red*). The *inset* shows a magnified image of a representative EdU labeled nuclei and ATP4A labeled cells. *B*, MUC5AC, a pit cell marker (*red*). *C*, GIF, gastric intrinsic factor, a chief cell marker (*red*). *D*, AGR2, expressed by mucous neck cells in *Agr2* WT (*red*) and EdU (*green*). The *inset* shows a magnified representative image of cells labeled for both AGR2 and EdU. Nuclei are stained blue with DAPI in all images. All *scale bars* represent 50 μm.

nuclear-labeled SOX9 cells were largely distinct from the proliferating cells, although the number of Ki-67- and SOX9-co-labeled cells increased by 3.3-fold per crypt in the *Agr2* KO.

Endoplasmic Reticulum Stress Response Genes Are Not Induced in Agr2 KO Mice—AGR2 protein resides and functions in the endoplasmic reticulum (ER) (43). A previous study of *Agr2* null mice detected enhanced expression of genes associated with the ER stress response (42). Examination of the ER stress response genes *Hspa5* and *Herpud1* by qRT-PCR in *Agr2* WT and KO mouse stomachs revealed no significant change (Table 1). As a positive control, ER stress was induced with tunicamycin in the mouse lung adenocarcinoma cell line, 394T4, which resulted in a 21- and 25-fold increase in *Hspa5* and *Herpud1* transcripts, respectively.

Analysis of Gene Expression with DNA Microarrays—RNA derived from the whole stomach of *Agr2* WT and *Agr2* KO mice were analyzed with respect to gene expression using DNA microarrays. For selected genes, confirmation was obtained by qRT-PCR (Table 1). Gene expression analysis revealed 858 genes that showed at least a 3-fold or more change in gene expression in the *Agr2* KO *versus* the *Agr2* WT stomach (GEO accession GSE40062). Many of the 486 genes whose expression declined were associated with the differentiated features of specific cell lineages as previously described. In contrast, 372 genes were enhanced 3-fold or more in the *Agr2* KO, which included transcripts for members of the *Reg* family of genes, *Reg1*, *Reg3A*, and *Reg3G* (Table 1).

DISCUSSION

The *in vivo* function for *Agr2* was explored using both constitutive and inducible conditional *Agr2* null mice. Constitutive *Agr2* loss resulted in a consistent phenotype featuring hyperplasia of the glandular stomach and premature death that was presumed secondary to gastric outlet obstruction. Histologic analysis of the *Agr2* KO mouse revealed an expansion in the number of cells expressing the mucous neck cell markers TFF2/GSII in the corpus and antrum. The same TFF2/GSII-positive cells were found to express AGR2 in the stomach of *Agr2* WT mice, indicating that *Agr2* expression regulates the number of mucous neck cells and deep antral gland cells.

In addition to the expansion of TFF2/GSII positive cells, the maturation of mucous neck cells to chief cells was perturbed. *Agr2* KO mice displayed persistent labeling by GSII lectin of chief cells at the bottom of the gland base, a feature usually lost with postnatal development of the gastric glands (5, 6, 12, 44).

The increase in TFF2/GSII-labeled cells observed in this study is similar to previous findings in which parietal cells were destroyed using drugs or toxins or through infection with *Helicobacter felis* (44–47). These models also expressed signs of incomplete maturation or metaplasia of chief cells characterized by TFF2/GSII labeling of cells in the gastric gland base and a decrease in intrinsic factor expression. Although not directly targeted, the number of parietal cells in the *Agr2* KO mice also a exhibited substantial decline with age compared with the *Agr2* WT mice. The constellation of features that include incomplete maturation of chief cells, loss of parietal cells, and expansion of TFF2/GSII-positive cells in the *Agr2* KO mice were similar to those previously described for a preneoplastic entity known as spasmolytic protein expressing metaplasia (SPEM) (47–49). Additional evidence that *Agr2* may contribute to the development of SPEM was obtained from the tamoxifen-treated

FIGURE 6. **Determination of cell proliferation in constitutive and inducible *Agr2* KO mice.** *A*, shown is labeling of the corpus (*left*) and antrum (*right*) of *Agr2* WT (*top panel*) and *Agr2* KO (*bottom panel*) mice with GSII lectin (*red*) and EdU (*green*) for proliferation. Tissue was harvested 2 and 15 h after EdU administration. Note that the bulk of EdU labeling is above the GSII layer, which is consistent with the isthmus layer. *B*, shown is quantitation of proliferating cells 2 and 15 h post-EdU labeling by counting EdU labeled cells as a percentage of the total number of nuclei (*left graph*). The total nuclei number is listed below the chart. The absolute number of EdU labeled cells per microscopic field (~590 μm of mucosal length/field) was also plotted (*right graph*). *C*, shown is labeling of the corpus (*left*) and antrum (*right*) for AGR2 (*red*) and the proliferation marker Ki-67 (*green*) of 8-week-old tamoxifen-treated $Agr2^{LoxP/LoxP}$ (*top*) and $Agr2^{LoxP/LoxP}$:*CMV-Cre*^{ERT2} (inducible KO, *bottom*) mice. The *white arrows* indicate representative AGR2-positive cells at the gland base. *D*, shown is quantitation of AGR2 (*top graphs*)- and Ki-67 (*bottom graphs*)-labeled cells in the inducible *Agr2* KO mouse as a percentage of the total nuclei number (*left graphs*) or the absolute number of labeled cells per field (*right graphs*). The total number of nuclei counted is listed *below the left graph*. *Error bars* for all charts represent ± 1 S.D. Nuclei are stained blue with DAPI in all the immunofluorescence images. All *scale bars* represent 50 μm.

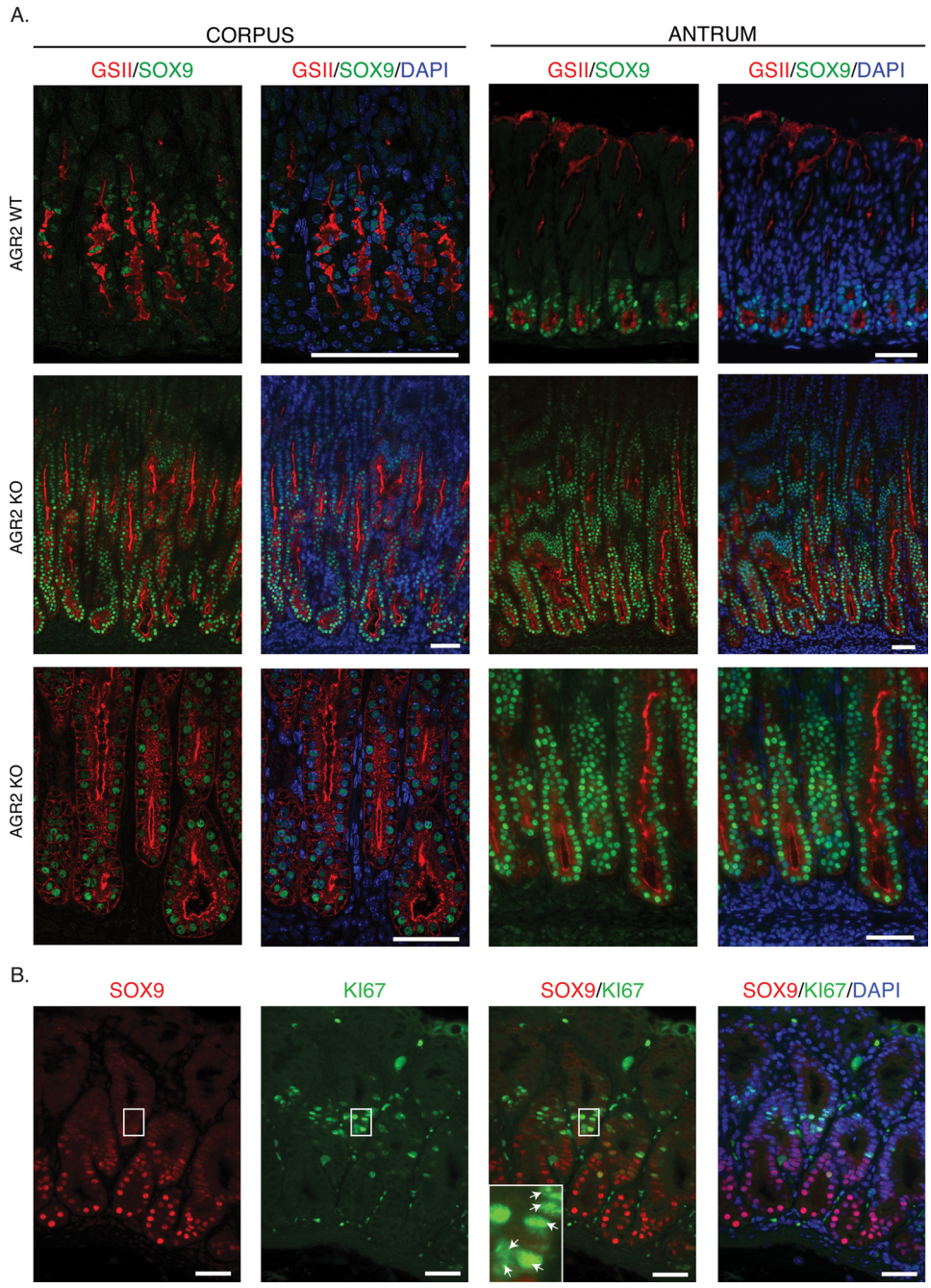

FIGURE 8. **Nuclear SOX9 positive cell numbers increase in the *Agr2* KO and is co-expressed with GSII.** *A*, 3-week-old *Agr2* WT (*top row*) and *Agr2* KO (*middle* and *bottom row*) mice were labeled with anti-SOX9 antisera (*green*) and GSII lectin (*red*) and DAPI stain for the nucleus (*blue*). The *bottom row* represents a magnified image showing co-labeling of SOX9 and GSII. The *Agr2* WT corpus is shown at higher magnification because the nuclear SOX9 signal was much less intense than the antrum. *B*, *Agr2* KO antrum labeled with antisera for SOX9 (*red*) and Ki-67 (*green*) is shown. The *inset* contains a magnified view of the area within the *white rectangle* showing double-labeled nuclei with Ki-67 and SOX9 (*arrows*). Proliferating $SOX9^{+}$ cells generally label less intensely. The nuclei are stained with DAPI in all images. The *scale bars* represent 50 μm.

$Agr2^{LoxP/LoxP}$ controls (Fig. 6*C*). Tamoxifen is known to induce a reversible metaplasia similar to SPEM. The control $Agr2^{LoxP/LoxP}$ mice expressed AGR2 in the same metaplastic cells that expressed GSII in the gastric gland base, thus supporting a potential role for *Agr2* in the development of SPEM. Although the observed hyperplasia in the *Agr2* KO mouse did not express signs of overt transformation with the formation of metastatic tumors, the features exhibited by the *Agr2* KO support a role for *Agr2* in the development of neoplasia.

The absence of *Agr2* expression resulted in a significant increase in cell proliferation. Increased cell proliferation was observed in both the stomach and intestinal tract and thus reflects what is likely a universal function for *Agr2*. Most proliferating cells were located in the gastric isthmus region and were unlabeled by any specific lineage marker, suggesting they may be stem cells or early progenitors. Because a definitive marker for stem cells in the gastric corpus has yet to be identified, the hypothesis is inferred from previous studies that have impli-

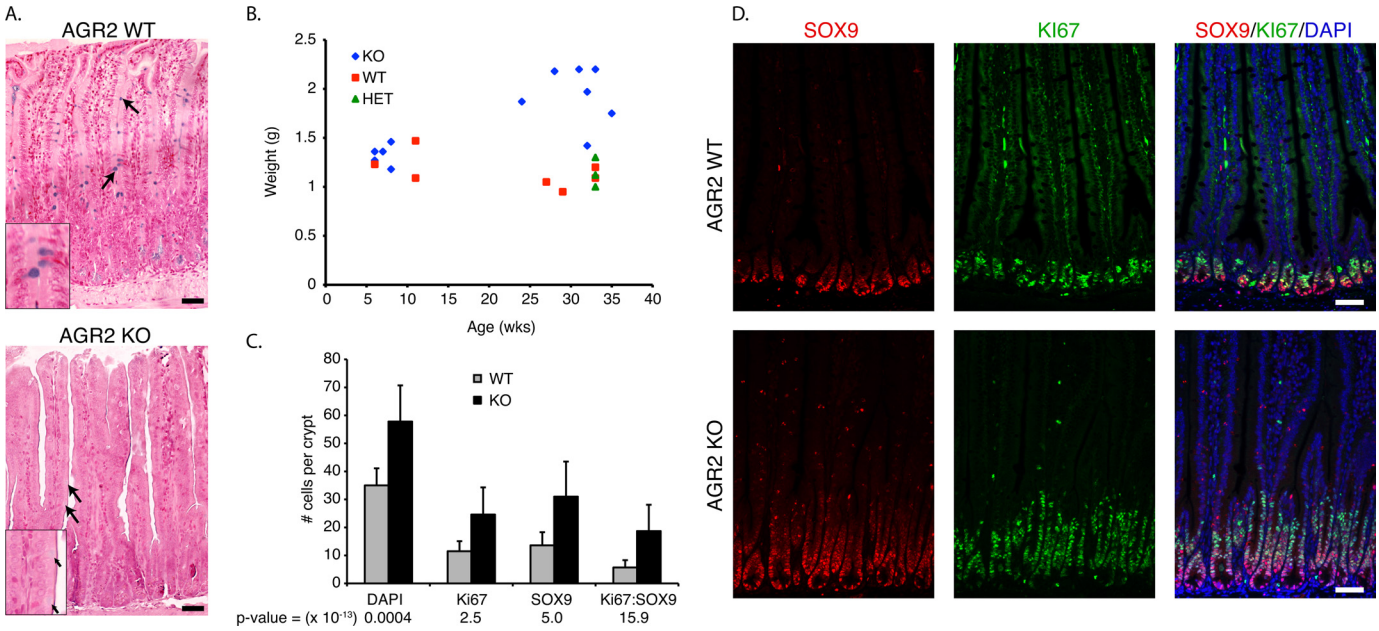

FIGURE 9. **The small intestine of *Agr2* KO mice exhibit decreased mucin and increased weight, cell proliferation, and nuclear SOX9.** *A*, hematoxylin and eosin stained the small intestine of *Agr2* WT and KO mice. Mucus-secreting goblet cells are stained with Alcian blue. The *arrows* highlight Alcian blue-stained goblet cells, and a magnified view is displayed in the *inset*. *B*, shown is a scatter plot of mouse age *versus* small intestine weight of *Agr2* KO (*KO*), WT (*WT*), and heterozygotes (*HET*). *C*, shown is the average number of SOX9- and Ki-67-labeled cells per crypt (*WT*, $n = 41$ crypts; *KO*, $n = 51$). *p* values ($\times 10^{-13}$) between WT and KO are listed below each measured label. *Error bars* represent $\pm$ 1 S.D. *D*, double-labeled immunofluorescence for SOX9 (*red*) and Ki-67 (*green*) is shown. The nuclei are stained blue with DAPI. The *scale bar* in all images represents 50 μm.

cated the isthmus as the source of gastric stem cells. Cell proliferation in the intestine was greatest in the mid-crypt, which is most consistent with the proliferation of progenitor cells. The results support a model in which *Agr2* expression results in negative feedback for cell proliferation. The results observed with the inducible *Agr2* KO in adult mice established that *Agr2* also regulates cell proliferation in the mature adult mice.

The results concerning cell proliferation may be viewed as contrary to previously published data in which *Agr2* enhanced the growth and cell division of adenocarcinoma cell lines. Previous work demonstrated that *Agr2* expression activates the Hippo and EGF signaling pathways in lung and esophageal adenocarcinoma cell lines (28). These results may be reconciled if there are different stimuli for cell division among stem cells and progenitors. In the wild-type animal, *Agr2* expression may promote cell division in a post-stem cell compartment while at the same time providing a negative feedback for an earlier compartment such as stem cells or early progenitors.

Agr2 exhibits other characteristics consistent with a role in a post-stem cell compartment, including the maturation of cell lineages. Gastric chief cells in the *Agr2* KO never fully develop. In the intestine, mucin-secreting goblet cells are present, but the mucin content is markedly decreased. The findings were similar to a recent study focused on intestinal goblet cell development in zebrafish, which concluded that *Agr2* serves a role in terminal differentiation (50). Similar to the present study, reduced zebrafish *Agr2* expression resulted in decreased mucin production without an actual change in goblet cell numbers.

The *Agr2* KO progressively expressed lower transcript levels for the products of enteroendocrine cells and mucin-secreting pit cells in the postnatal period. In addition, parietal cells also declined in numbers as the mouse aged. The result suggests that *Agr2* loss results in incomplete maturation of chief cells and compromises the persistence or maturation of other differentiated cell lineages. Previous studies have demonstrated that disruption of one lineage can affect the homeostasis and maintenance of other lineages in the stomach (44–47). Another potential cause for the delayed effects on parietal-, enteroendocrine-, and mucin-secreting cells may be the postnatal development of the gastric glands. Complete development as characterized by attainment of full thickness of the gastric glands is not achieved until 6 weeks of age in the mouse. The full impact of the *Agr2* null may not be achieved until 6 weeks when the gastric glands are fully developed and *Agr2* may be fully functional in the newly established mucous neck cells. How *Agr2* affects other cell lineages remains unclear and is a focus of current investigations.

The decline in intestinal goblet cell mucin observed in this study was similar to two previous publications that also generated *Agr2* null mice. One study by Park *et al.* (41) attributed the decrease in intestinal mucus production to a role for *Agr2* in MUC2 folding as supported by its *in vitro* binding to AGR2 protein (42).

In contrast to the study by Zhao *et al.* (42), this study and that of Park *et al.* (41) did not result in an increase in inflammation or ER stress response. It should be noted that the mice in the study by Park *et al.* (41) were housed in a gnotobiotic facility. A recent zebrafish study also found no evidence of an increased ER stress response with the reduction in *Agr2* expression (50), a result shared by the *Agr2* KO mice in this study.

Clearly the most profound difference between this study and the two previously published *Agr2* null mice were the effects observed in the stomach. No abnormalities were previously reported in the stomach. The reasons for the differences are unclear, although all three studies generated the *Agr2* null mice using different targeting constructs, promoters for the expression of Cre recombinase, and

husbandry conditions. Similar to this study, Park *et al.* (41) did report weight loss by the *Agr2* null mice beginning at 16 weeks, which were followed to 21 weeks. In contrast, the *Agr2* KO mice in this study were followed for up to 36 weeks, and significant morbidity requiring euthanasia was encountered at 26 weeks.

The DNA microarray analysis supported a significant regulatory role for *Agr2*, which revealed changes in expression of 3-fold or more for >800 genes in the *Agr2* KO. Previous work determined that AGR2 protein functions from within the endoplasmic reticulum (43), which may mediate the assembly or folding of yet to be defined regulatory proteins that reside or are in transit through the ER. Among the genes identified by the DNA microarrays were members of the *Reg* family of genes, which have been previously implicated in promoting gastric mucosal growth. Enhanced *Reg1* expression has been implicated in gastric regeneration and the expansion of progenitor cells in the neck zone (51, 52) and in human preneoplastic and neoplastic lesions (53, 54).

Agr2 loss results in incomplete maturation of chief cells and a decline in other differentiated cell lineages. The persistence of immature cells that do not fully mature is also supported by the expansion of nuclear SOX9-labeled cells in the *Agr2* KO mice. Previous work has shown that *Sox9* can deter maturation and may serve to maintain the pluripotent state of stem or progenitor cells (38). Recent studies have also shown that *Sox9* is expressed in proliferating stem cells (55), which provides insight into the significant fraction of proliferating cells that are SOX9-positive in this study (Figs. 8 and 9). Furthermore, mucous neck cells and deep antral gland cells in the normal glandular stomach expressed AGR2 and SOX9, and the absence of *Agr2* expression results in the expansion of GSII/SOX9-labeled cells, some of which are actively proliferating (Fig. 4*A*). The co-expression with *Sox9* indicates that *Agr2* is expressed in cells that may represent an immature progenitor before terminal differentiation and is consistent with prior studies (9). The data also indicate that *Agr2* may affect the fate of cells that do not ultimately express the gene.

Prior studies describing a *Sox9* null mutation that was specifically induced in the intestine shared many features with that of the *Agr2* KO mouse described in the present study (56). The absence of intestinal *Sox9* expression constrained the maturation of goblet cells and led to an increase in intestinal cell proliferation, hyperplasia, and dysplasia. The phenotypes of the *Agr2* and *Sox9* null mutants indicate that the expression of either gene results in negative feedback inhibition of cell proliferation. Considering the significant increase in nuclear SOX9 observed in the *Agr2* KO stomach and intestine, *Agr2* may function downstream of *Sox9*. In fact, a recently published gene expression profile demonstrated that induced expression of *Sox9* in HT-29 cells by transfection significantly enhanced *Agr2* expression (57).

This study supports a role for *Agr2* in regulating cell homeostasis at the level of stem/early progenitor cell proliferation, which is operational in adult mice. *Agr2* expression influences cell lineage maturation. *Agr2* is also expressed in metaplasia, and disrupted *Agr2* expression results in many features consistent with a preneoplastic process for stomach cancer.

Acknowledgments—We appreciate Aiwen Dong and Christine Cartwright for critical reading of the manuscript.

REFERENCES

1. Lee, E. R., Trasler, J., Dwivedi, S., and Leblond, C. P. (1982) Division of the mouse gastric mucosa into zymogenic and mucous regions on the basis of gland features. *Am. J. Anat.* **164,** 187–207
2. Karam, S. M., and Leblond, C. P. (1993) Dynamics of epithelial cells in the corpus of the mouse stomach. I. Identification of proliferative cell types and pinpointing of the stem cell. *Anat. Rec.* **236,** 259–279
3. Bjerknes, M., and Cheng, H. (2002) Multipotential stem cells in adult mouse gastric epithelium. *Am. J. Physiol. Gastrointest. Liver Physiol.* **283,** G767–G777
4. Mills, J. C., and Shivdasani, R. A. (2011) Gastric epithelial stem cells. *Gastroenterology* **140,** 412–424
5. Keeley, T. M., and Samuelson, L. C. (2010) Cytodifferentiation of the postnatal mouse stomach in normal and Huntingtin-interacting protein 1-related-deficient mice. *Am. J. Physiol. Gastrointest Liver Physiol.* **299,** G1241–G1251
6. Karam, S. M., Li, Q., and Gordon, J. I. (1997) Gastric epithelial morphogenesis in normal and transgenic mice. *Am. J. Physiol.* **272,** G1209–G1220
7. Ramsey, V. G., Doherty, J. M., Chen, C. C., Stappenbeck, T. S., Konieczny, S. F., and Mills, J. C. (2007) The maturation of mucus-secreting gastric epithelial progenitors into digestive-enzyme secreting zymogenic cells requires Mist1. *Development* **134,** 211–222
8. Kataoka, K., Takeoka, Y., and Furihata, C. (1990) Immunocytochemical study of pepsinogen 1-producing cells in the fundic mucosa of the stomach in developing mice. *Cell Tissue Res.* **261,** 211–217
9. Quante, M., Marrache, F., Goldenring, J. R., and Wang, T. C. (2010) TFF2 mRNA transcript expression marks a gland progenitor cell of the gastric oxyntic mucosa. *Gastroenterology* **139,** 2018–2027
10. Jeffrey, G. P., Oates, P. S., Wang, T. C., Babyatsky, M. W., and Brand, S. J. (1994) Spasmolytic polypeptide. A trefoil peptide secreted by rat gastric mucous cells. *Gastroenterology* **106,** 336–345
11. Ebisu, S., and Goldstein, I. J. (1978) *Bandeiraea simplicifolia* lectin II. *Methods Enzymol.* **50,** 350–354
12. Ihida, K., Suganuma, T., Tsuyama, S., and Murata, F. (1988) Glycoconjugate histochemistry of the rat fundic gland using *Griffonia simplicifolia* agglutinin-II during the development. *Am. J. Anat.* **182,** 250–256
13. Oinuma, T., Kawano, J., and Suganuma, T. (1991) Glycoconjugate histochemistry of *Xenopus laevis* fundic gland with special reference to mucous neck cells during development. *Anat. Rec.* **230,** 502–512
14. Hao, Y., Triadafilopoulos, G., Sahbaie, P., Young, H. S., Omary, M. B., and Lowe, A. W. (2006) Gene expression profiling reveals stromal genes expressed in common between Barrett's esophagus and adenocarcinoma. *Gastroenterology* **131,** 925–933
15. Lowe, A. W., Olsen, M., Hao, Y., Lee, S. P., Taek Lee, K., Chen, X., van de Rijn, M., and Brown, P. O. (2007) Gene expression patterns in pancreatic tumors, cells, and tissues. *PLoS ONE* **2,** e323
16. Thompson, D. A., and Weigel, R. J. (1998) hAG-2, the human homologue of the *Xenopus laevis* cement gland gene XAG- 2, is coexpressed with estrogen receptor in breast cancer cell lines. *Biochem. Biophys. Res. Commun.* **251,** 111–116
17. Zhang, J. S., Gong, A., Cheville, J. C., Smith, D. I., and Young, C. Y. (2005) AGR2, an androgen-inducible secretory protein overexpressed in prostate cancer. *Genes Chromosomes Cancer* **43,** 249–259
18. Fritzsche, F. R., Dahl, E., Dankof, A., Burkhardt, M., Pahl, S., Petersen, I., Dietel, M., and Kristiansen, G. (2007) Expression of AGR2 in non small cell lung cancer. *Histology and Histopathology* **22,** 703–708
19. Zhu, H., Lam, D. C., Han, K. C., Tin, V. P., Suen, W. S., Wang, E., Lam, W. K., Cai, W. W., Chung, L. P., and Wong, M. P. (2007) High resolution analysis of genomic aberrations by metaphase and array comparative genomic hybridization identifies candidate tumour genes in lung cancer cell lines. *Cancer Lett.* **245,** 303–314
20. Edgell, T. A., Barraclough, D. L., Rajic, A., Dhulia, J., Lewis, K. J., Armes, J. E., Barraclough, R., Rudland, P. S., Rice, G. E., and Autelitano, D. J. (2010) Increased plasma concentrations of anterior gradient 2 protein are positively associated with ovarian cancer. *Clin. Sci.* **118,** 717–725
21. Lee, S., Bang, S., Song, K., and Lee, I. (2006) Differential expression in normal-adenoma-carcinoma sequence suggests complex molecular carcinogenesis in colon. *Oncol. Rep.* **16,** 747–754

22. Bai, Z., Ye, Y., Liang, B., Xu, F., Zhang, H., Zhang, Y., Peng, J., Shen, D., Cui, Z., Zhang, Z., and Wang, S. (2011) Proteomics-based identification of a group of apoptosis-related proteins and biomarkers in gastric cancer. *Int. J. Oncol.* **38,** 375–383
23. Aberger, F., Weidinger, G., Grunz, H., and Richter, K. (1998) Anterior specification of embryonic ectoderm. The role of the *Xenopus* cement gland-specific gene XAG-2. *Mech. Dev.* **72,** 115–130
24. Sive, H. L., Hattori, K., and Weintraub, H. (1989) Progressive determination during formation of the anteroposterior axis in *Xenopus laevis*. *Cell* **58,** 171–180
25. Kumar, A., Godwin, J. W., Gates, P. B., Garza-Garcia, A. A., and Brockes, J. P. (2007) Molecular basis for the nerve dependence of limb regeneration in an adult vertebrate. *Science* **318,** 772–777
26. Liu, D., Rudland, P. S., Sibson, D. R., Platt-Higgins, A., and Barraclough, R. (2005) Human homologue of cement gland protein, a novel metastasis inducer associated with breast carcinomas. *Cancer Res.* **65,** 3796–3805
27. Wang, Z., Hao, Y., and Lowe, A. W. (2008) The adenocarcinoma-associated antigen, AGR2, promotes tumor growth, cell migration, and cellular transformation. *Cancer Res.* **68,** 492–497
28. Dong, A., Gupta, A., Pai, R. K., Tun, M., and Lowe, A. W. (2011) The human adenocarcinoma-associated gene, AGR2, induces expression of amphiregulin through Hippo pathway coactivator YAP1 activation. *J. Biol. Chem.* **286,** 18301–18310
29. Huh, W. J., Khurana, S. S., Geahlen, J. H., Kohli, K., Waller, R. A., and Mills, J. C. (2012) Tamoxifen induces rapid, reversible atrophy, and metaplasia in mouse stomach. *Gastroenterology* **142,** 21–24
30. Madsen, J., Nielsen, O., Tornøe, I., Thim, L., and Holmskov, U. (2007) Tissue localization of human trefoil factors 1, 2, and 3. *J. Histochem. Cytochem.* **55,** 505–513
31. Salic, A., and Mitchison, T. J. (2008) A chemical method for fast and sensitive detection of DNA synthesis *in vivo*. *Proc. Natl. Acad. Sci. U.S.A.* **105,** 2415–2420
32. Workman, C., Jensen, L. J., Jarmer, H., Berka, R., Gautier, L., Nielser, H. B., Saxild, H. H., Nielsen, C., Brunak, S., and Knudsen, S. (2002) A new non-linear normalization method for reducing variability in DNA microarray experiments. *Genome Biol.* **3,** research0048
33. Reich, M., Liefeld, T., Gould, J., Lerner, J., Tamayo, P., and Mesirov, J. P. (2006) GenePattern 2.0. *Nat. Genet.* **38,** 500–501
34. Lefebvre, O., Wolf, C., Kédinger, M., Chenard, M. P., Tomasetto, C., Chambon, P., and Rio, M. C. (1993) The mouse one P-domain (pS2) and two P-domain (mSP) genes exhibit distinct patterns of expression. *J. Cell Biol.* **122,** 191–198
35. Gerdes, J., Lemke, H., Baisch, H., Wacker, H. H., Schwab, U., and Stein, H. (1984) Cell cycle analysis of a cell proliferation-associated human nuclear antigen defined by the monoclonal antibody Ki-67. *J. Immunol.* **133,** 1710–1715
36. Sashikawa Kimura, M., Mutoh, H., and Sugano, K. (2011) SOX9 is expressed in normal stomach, intestinal metaplasia, and gastric carcinoma in humans. *J. Gastroenterol.* **46,** 1292–1299
37. Furuyama, K., Kawaguchi, Y., Akiyama, H., Horiguchi, M., Kodama, S., Kuhara, T., Hosokawa, S., Elbahrawy, A., Soeda, T., Koizumi, M., Masui, T., Kawaguchi, M., Takaori, K., Doi, R., Nishi, E., Kakinoki, R., Deng, J. M., Behringer, R. R., Nakamura, T., and Uemoto, S. (2011) Continuous cell supply from a Sox9-expressing progenitor zone in adult liver, exocrine pancreas. and intestine. *Nat. Genet.* **43,** 34–41
38. Seymour, P. A., Freude, K. K., Tran, M. N., Mayes, E. E., Jensen, J., Kist, R., Scherer, G., and Sander, M. (2007) SOX9 is required for maintenance of the pancreatic progenitor cell pool. *Proc. Natl. Acad. Sci. U.S.A.* **104,** 1865–1870
39. Vidal, V. P., Chaboissier, M. C., Lützkendorf, S., Cotsarelis, G., Mill, P., Hui, C. C., Ortonne, N., Ortonne, J. P., and Schedl, A. (2005) Sox9 is essential for outer root sheath differentiation and the formation of the hair stem cell compartment. *Curr. Biol.* **15,** 1340–1351
40. Nowak, J. A., Polak, L., Pasolli, H. A., and Fuchs, E. (2008) Hair follicle stem cells are specified and function in early skin morphogenesis. *Cell Stem Cell* **3,** 33–43
41. Park, S. W., Zhen, G., Verhaeghe, C., Nakagami, Y., Nguyenvu, L. T., Barczak, A. J., Killeen, N., and Erle, D. J. (2009) The protein disulfide isomerase AGR2 is essential for production of intestinal mucus. *Proc. Natl. Acad. Sci. U.S.A.* **106,** 6950–6955
42. Zhao, F., Edwards, R., Dizon, D., Afrasiabi, K., Mastroianni, J. R., Geyfman, M., Ouellette, A. J., Andersen, B., and Lipkin, S. M. (2010) Disruption of Paneth and goblet cell homeostasis and increased endoplasmic reticulum stress in $Agr2^{-/-}$ mice. *Dev. Biol.* **338,** 270–279
43. Gupta, A., Dong, A., and Lowe, A. W. (2012) AGR2 gene function requires a unique endoplasmic reticulum localization motif. *J. Biol. Chem.* **287,** 4773–4782
44. Nozaki, K., Ogawa, M., Williams, J. A., Lafleur, B. J., Ng, V., Drapkin, R. I., Mills, J. C., Konieczny, S. F., Nomura, S., and Goldenring, J. R. (2008) A molecular signature of gastric metaplasia arising in response to acute parietal cell loss. *Gastroenterology* **134,** 511–522
45. Nam, K. T., Lee, H. J., Sousa, J. F., Weis, V. G., O'Neal, R. L., Finke, P. E., Romero-Gallo, J., Shi, G., Mills, J. C., Peek, R. M., Jr., Konieczny, S. F., and Goldenring, J. R. (2010) Mature chief cells are cryptic progenitors for metaplasia in the stomach. *Gastroenterology* **139,** 2028–2037
46. Li, Q., Karam, S. M., and Gordon, J. I. (1996) Diphtheria toxin-mediated ablation of parietal cells in the stomach of transgenic mice. *J. Biol. Chem.* **271,** 3671–3676
47. Nomura, S., Yamaguchi, H., Ogawa, M., Wang, T. C., Lee, J. R., and Goldenring, J. R. (2005) Alterations in gastric mucosal lineages induced by acute oxyntic atrophy in wild-type and gastrin-deficient mice. *Am. J. Physiol. Gastrointest. Liver Physiol.* **288,** G362–G375
48. Goldenring, J. R., Nam, K. T., Wang, T. C., Mills, J. C., and Wright, N. A. (2010) Spasmolytic polypeptide-expressing metaplasia and intestinal metaplasia. Time for reevaluation of metaplasias and the origins of gastric cancer. *Gastroenterology* **138,** 2207–2210
49. Schmidt, P. H., Lee, J. R., Joshi, V., Playford, R. J., Poulsom, R., Wright, N. A., and Goldenring, J. R. (1999) Identification of a metaplastic cell lineage associated with human gastric adenocarcinoma. *Lab. Invest.* **79,** 639–646
50. Chen, Y. C., Lu, Y. F., Li, I. C., and Hwang, S. P. (2012) Zebrafish agr2 is required for terminal differentiation of intestinal goblet cells. *PLoS ONE* **7,** e34408
51. Fukuhara, H., Kadowaki, Y., Ose, T., Monowar, A., Imaoka, H., Ishihara, S., Takasawa, S., and Kinoshita, Y. (2010) *In vivo* evidence for the role of RegI in gastric regeneration. Transgenic overexpression of RegI accelerates the healing of experimental gastric ulcers. *Lab. Invest.* **90,** 556–565
52. Miyaoka, Y., Kadowaki, Y., Ishihara, S., Ose, T., Fukuhara, H., Kazumori, H., Takasawa, S., Okamoto, H., Chiba, T., and Kinoshita, Y. (2004) Transgenic overexpression of Reg protein caused gastric cell proliferation and differentiation along parietal cell and chief cell lineages. *Oncogene* **23,** 3572–3579
53. Yamaoka, T., Yoshino, K., Yamada, T., Idehara, C., Hoque, M. O., Moritani, M., Yoshimoto, K., Hata, J., and Itakura, M. (2000) Diabetes and tumor formation in transgenic mice expressing Reg I. *Biochem. Biophys. Res. Commun.* **278,** 368–376
54. Steele, I. A., Dimaline, R., Pritchard, D. M., Peek, R. M., Jr., Wang, T. C., Dockray, G. J., and Varro, A. (2007) *Helicobacter* and gastrin stimulate Reg1 expression in gastric epithelial cells through distinct promoter elements. *Am. J. Physiol. Gastrointest. Liver Physiol.* **293,** G347–G354
55. Formeister, E. J., Sionas, A. L., Lorance, D. K., Barkley, C. L., Lee, G. H., and Magness, S. T. (2009) Distinct SOX9 levels differentially mark stem/progenitor populations and enteroendocrine cells of the small intestine epithelium. *Am. J. Physiol. Gastrointest. Liver Physiol.* **296,** G1108–G1118
56. Mori-Akiyama, Y., van den Born, M., van Es, J. H., Hamilton, S. R., Adams, H. P., Zhang, J., Clevers, H., and de Crombrugghe, B. (2007) SOX9 is required for the differentiation of paneth cells in the intestinal epithelium. *Gastroenterology* **133,** 539–546
57. Zalzali, H., Naudin, C., Bastide, P., Quittau-Prévostel, C., Yaghi, C., Poulat, F., Jay, P., and Blache, P. (2008) CEACAM1, a SOX9 direct transcriptional target identified in the colon epithelium. *Oncogene* **27,** 7131–7138
58. Lee, E. R. (1985) Dynamic histology of the antral epithelium in the mouse stomach. I. Architecture of antral units. *Am. J. Anat.* **172,** 187–204